Calcium Occupancy of N-Terminal Sites within Calmodulin Induces Inhibition of the Ryanodine Receptor Calcium Release Channel†

Curt B. Boschek, Terry E. Jones,‡ Thomas C. Squier, and Diana J. Bigelow*

Cell Biology and Biochemistry Group, Biological Sciences Division, Pacific Northwest National Laboratory, Richland, Washington 99352

Received April 6, 2007; Revised Manuscript Received July 11, 2007

ABSTRACT: Calmodulin (CaM) regulates calcium release from intracellular stores in skeletal muscle through its association with the ryanodine receptor (RyR1) calcium release channel, where CaM association enhances channel opening at resting calcium levels and its closing at micromolar calcium levels associated with muscle contraction. A high-affinity CaM-binding sequence (RyRp) has been identified in RyR1, which corresponds to a 30-residue sequence (i.e., $K^{3614}-N^{3643}$) located within the central portion of the primary sequence. However, it is presently unclear whether the identified CaM-binding sequence in association with CaM (a) senses calcium over the physiological range of calcium concentrations associated with RyR1 regulation or alternatively, (b) plays a structural role unrelated to the calcium-dependent modulation of RyR1 function. Therefore, we have measured the calcium-dependent activation of the individual domains of CaM in association with RyRp and their relationship to the CaM-dependent regulation of RyR1. These measurements utilize an engineered CaM, permitting the site-specific incorporation of *N*-(1-pyrene)-maleimide at either T34C (Py_N-CaM) or T110C (Py_C-CaM) in the N- and C-domains, respectively. Consistent with prior measurements, we observe a high-affinity association of both apo-CaM and calcium-activated CaM with RyRp. Upon association with RyRp, fluorescence changes in Py_N-CaM or Py_C-CaM permit the measurement of the calcium-dependent activation of these individual domains. Fluorescence changes upon calcium activation of Py_C-CaM in association with RyRp are indicative of high-affinity calcium-dependent activation of the C-terminal domain of CaM at resting calcium levels; at calcium levels associated with muscle contraction, activation of the N-terminal domain occurs with concomitant increases in the fluorescence intensity of Py_C-CaM that is associated with structural changes within the CaM-binding sequence of RyR1. Occupancy of calcium-binding sites in the N-domain of CaM mirrors the calcium dependence of RyR1 inhibition observed at activating calcium levels, where $[Ca]_{1/2} = 4.3 \pm 0.4$ μM, suggesting a direct regulation of RyR1 function upon the calcium-dependent activation of CaM. These results indicate that occupancy of the N-terminal domain calcium binding sites in CaM bound to the identified CaM-binding sequence $K^{3614}-N^{3643}$ induces conformational rearrangements within the complex between CaM and RyR1 responsible for the CaM-dependent modulation of the RyR1 calcium release channel.

Ryanodine receptor (RyR1)[1] calcium release channels in skeletal muscle are responsible for calcium-induced calcium release from the sarcoplasmic reticulum (SR), which initiates muscle contraction. RyR1 is a large homotetrameric channel for which each 565 kDa subunit includes a single known high-affinity calmodulin (CaM) binding site (*1*−*4*). Functional assays of RyR1 channel opening indicate a bell-shaped calcium dependency that is modulated by CaM association, which acts to enhance channel opening at low (i.e., submicromolar) calcium concentrations and facilitate channel closing at the micromolar calcium levels associated with muscle contraction (*5*, *6*). CaM bound to each subunit of RyR1 has been visualized by cryoelectron microscopy (cryo-EM) image reconstructions and shown to undergo calcium-dependent positional shifts with respect to the structure of RyR1 (*7*).

A highly conserved CaM-binding sequence (i.e., $K^{3614}-N^{3643}$ in RyR1) that binds both apo-CaM and calcium-activated CaM with high affinity is present in all vertebrate ryanodine receptors, and mutations within this

† This work was supported by NIH Grants AG12993 and AG18013. Pacific Northwest National Laboratory is operated for the US DOE by Battelle Memorial Institute under Contract DE-AC05-76RL0 1830.

* Correspondence should be addressed to this author: Cell Biology and Biochemistry Group, 790 6th St., Mail Stop P7-53, Pacific Northwest National Laboratory, Richland, WA 99354; tel (509) 376-2378; fax (509) 376-6767; e-mail diana.bigelow@pnl.gov.

‡ Present address: Department of Physical Therapy, School of Allied Health Sciences, East Carolina University, Greenville, NC 27858.

[1] Abbreviations: β-ME, 2-mercaptoethanol; BSA, bovine serum albumin; CaM, calmodulin; CHAPS, 3-[(3-cholamidopropyl)dimethylammonio]-1-propanesulfonic acid; DTT, dithiothreitol; EGTA, ethylene glycol bis(2-aminoethyl ether)-*N*,*N*,*N*′,*N*′-tetraacetic acid; HEPES, *N*-(2-hydroxyethyl)piperazine-*N*′-2-ethanesulfonic acid; HSR, heavy sarcoplasmic reticulum vesicles enriched in RyR1; IPTG, β-D-1-thiogalactopyranoside; MOPS, 3-(*N*-morpholino)propanesulfonic acid; MS, mass spectrometry; Py, pyrene; Py_N-CaM, *N*-(1-pyrene)maleimide-labeled T34C-calmodulin; Py_C-CaM, *N*-(1-pyrene)maleimide-labeled T110C-calmodulin; Py_2-CaM, T34C,T110C-calmodulin labeled at both introduced cysteines with *N*-(1-pyrene)maleimide; RyR1, ryanodine receptor; RyRp, peptide corresponding to residues 3614−3643 of ryanodine receptor; SDS−PAGE, sodium dodecyl sulfate−polyacrylamide gel electrophoresis; TCEP, tris(carboxyethyl)phosphine.

10.1021/bi700655h CCC: $37.00
Published on Web 08/22/2007

sequence affect the CaM-dependent regulation of RyR isoforms (*3*, *8*−*12*). Common to many CaM-binding sequences, this peptide contains a hydrophobic anchor (i.e., Trp^{3620}) that is required for high-affinity CaM binding (*10*, *13*−*15*). Indeed, the recently published high-resolution structure of calcium-activated CaM in complex with the peptide K^{3614}−N^{3643} (i.e., RyRp) demonstrates that the opposing domains of CaM wrap around the peptide in a manner similar to that observed for smooth muscle myosin light chain kinase (smMLCK), albeit with a larger distance between the opposing domains of CaM (*13*).

However, questions remain regarding the role of the identified RyR1 CaM binding sequence, RyRp, with respect to its role in mediating the enhanced calcium sensitivity of RyR1 following CaM binding. In this respect, a primary concern is recent reports that, upon association with this CaM-binding sequence, the calcium affinity of CaM is substantially enhanced, resulting in reported dissociation constants of either 81 ± 1 nM (*15*) or more recently 200 ± 100 nM (*16*). These K_d values suggest that the calcium-binding sites in CaM are essentially fully occupied near resting calcium levels, implying that the identified CaM-binding sequence is not sufficient to account for the enhanced calcium sensitivity of RyR1 following CaM binding. These results were interpreted to suggest that the CaM-dependent regulation of RyR1 requires either additional CaM binding site(s) or the involvement of other portions of the RyR1 calcium release channel (*17*). However, a single CaM is thought to associate with each subunit of RyR1 (*7*), and in the case of other target proteins the identical structures of CaM bound to either the intact protein or the peptide corresponding to the CaM-binding sequence suggests the regulatory involvement of only the CaM-binding sequence (*18*, *19*).

To clarify the potential role of the identified high-affinity CaM-binding sequence (RyRp) in modulating the calcium dependence of RyR1 channel activity, we have used an engineered CaM, permitting the site-specific incorporation of *N*-(1-pyrene)maleimide at either T34C (Py_N-CaM) or T110C (Py_C-CaM) in the N- and C-domains to examine the calcium-dependent activation of individual domains in CaM bound to RyRp. The engineered CaM sensors do not interfere with binding, as probe sites are highly solvent-exposed in CaM prior to and following association with the CaM-binding sequence of RyR1 calcium release channel (Figure 1). Furthermore, these constructs have been previously used to detect differences in the calcium-dependent activation of individual domains in CaM (*20*), and overcome limitations associated with earlier measurements where localized fluorescence changes at a single site were measured in response to calcium binding to CaM corresponding to either the fluorescence of Trp^{3620} in the CaM-binding peptide or acrylodan covalently bound to an engineered cysteine in the N-domain of CaM bound to RyRp (*15*, *16*). We find that the association of CaM with RyRp leads to a small increase in the affinities of the calcium binding sites in the N-terminal globular domain of CaM and that occupancy of these low-affinity calcium binding sites mirrors the calcium-dependent inactivation of RyR. These results suggest that calcium occupancy of the low-affinity calcium-binding sites in the N-terminal domain of CaM functions as the calcium sensor to promote RyR1 channel closure.

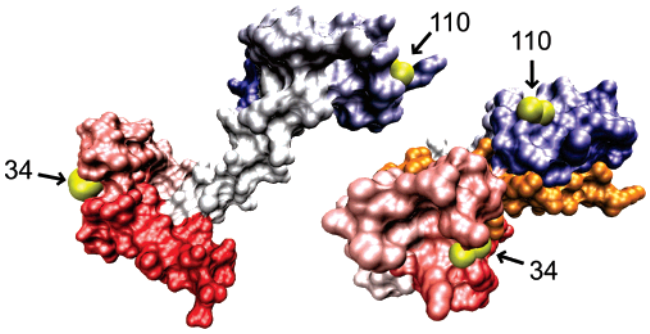

FIGURE 1: Highly solvent-accessible positions of pyrene labeling sites in CaM. Surface accessibilities of *N*-(1-pyrene)maleimide labeling sites (yellow) at positions 34 in the N-terminus and 110 the in C-terminus of CaM are shown in high-resolution structures for calcium-activated CaM (3CLN, left) and calcium-activated CaM in complex with RyRp (2BCX, right), where proteins are depicted as surfaces with van der Waals radii of 1.4 Å for all atoms. The CaM-binding sequence of RyR1 (i.e., RyRp) is orange; CaM is depicted as a color gradient from red (N-domain) to blue (C-domain).

EXPERIMENTAL PROCEDURES

Materials. [^{3}H]-ryanodine was obtained from New England Nuclear, Boston, MA; RyRp (KSKKAVWHKLLSKQRRRAVVACFRMTPLYN), the absolutely conserved peptide corresponding to the CaM-binding domain of RyR1 in all vertebrates (residues 3614−3643; NCBI no. P11716), was synthesized by SynPep (Dublin, CA). *Escherichia coli* BL21-(DE3) containing plasmids for CaM mutants containing either single cysteines in the N-domain (i.e., T34C) or C-domain (i.e., T110C) or two cysteines (i.e., T34C/T110C) was provided by Ramona Bieber-Urbauer (*21*) and was purified essentially as previously described (*22*, *23*). All other chemicals were the purest grade commercially available.

Isolation of HSR. Heavy SR vesicles corresponding to terminal cisternae of SR were prepared from F344BN hybrid rat hind limb muscles through a series of differential centrifugations essentially as described by Mickelson et al. (*24*) and Yang et al. (*25*). Flash-frozen muscle was thawed and homogenized at 5 mL/g in 0.1 M NaCl and 5 mM Tris maleate (pH 6.8), centrifuged at 3300*g* for 30 min, and the supernatant was then filtered through cheesecloth. The pellet resulting from centrifugation at 16300*g* for 30 min of the filtered supernatant was resuspended in 5 mM Tris maleate (pH 6.8), 0.3 M sucrose, 0.4 M KCl, and 20 μM $CaCl_2$ and subjected to a discontinuous sucrose density gradient of 22%, 35%, and 45% (w/v) and centrifuged at 112400*g* for 5 h. The HSR fraction at the 35%/45% interface was collected, diluted 4 times in 10% (w/v) sucrose and 5 mM Tris maleate (pH 6.8), and centrifuged at 181000*g* for 40 min. The resulting pellets were resuspended in a minimal volume of 10% (w/v) sucrose and 5 mM Tris maleate (pH 6.8) and stored at −80 °C. All solutions contained a protease inhibitor cocktail (0.1 mM phenymethanesulfonyl fluoride (PMSF) and 1 μg/mL each of aprotinin, benzamidine, leupeptin, and pepstatin).

[^{3}H]-Ryanodine Binding. Calcium concentration dependences of [^{3}H]ryanodine binding to HSR vesicles were assessed essentially as described by Zhang et al. (*26*). HSR vesicles were incubated in 50 mM MOPS (pH 7.4), 300 mM NaCl, 100 μg/mL BSA, 0.1% CHAPS, 0.7 mM EGTA, 20 nM [^{3}H]-ryanodine, and concentrations of $CaCl_2$ to elicit the

desired free calcium concentrations for 16−18 h at room temperature in the presence and absence of 10 μM unlabeled ryanodine to define nonspecific binding of [^{3}H]ryanodine. Free ryanodine was separated by filtration through Whatman GF/F glass fiber filters and five rinses of 3 mL of 50 nM MOPS (pH 7.4), 300 mM NaCl, 100 μg/mL BSA, 0.7 mM EGTA, and the appropriate amount of $CaCl_2$ to provide the desired free calcium concentration. The labeled protein was eluted from the filters by shaking for 60 min in 5 mL of ReadyPro+ scintillation fluid (Beckman, Fullerton, CA) and radioactivity was measured on a Packard TriCarb 2100TR (Packard, Downers Grove, IL). Specific binding of [^{3}H]-ryanodine to RyR1 was calculated by subtracting nonspecific binding from total binding.

Covalent Labeling of CaM with Pyrene. CaM was specifically labeled with pyrene in either domain as previously described (*20*, *21*). Briefly, CaM mutants (T34C-CaM or T110C-CaM) in 10 mM HEPES (pH 7.8) were reduced with 0.25 μM tris(carboxyethyl) phosphine (TCEP), and then a 20-fold molar excess of *N*-(1-pyrene)maleimide was added. After incubation for 2 h, excess dye was removed by use of a Sephadex G25 column. The stoichiometry of bound pyrene was measured by use of the extinction coefficient ϵ_{340} = 40 000 M^{-1} cm^{-1} (*27*).

Fluorescence Measurements. Emission spectra or anisotropy measurements were acquired at 25 °C on a FluoroLog2 Spex instrument (Horiba Jobin Yvon Inc.; Edison, NJ) at 1.0 nm resolution with both excitation and emission slits set at 5 nm. Excitation was at 295 nm or 330 nm for RyRp (1.1 μM) or Py_N- or Py_C-CaM (100 nM). In all cases, measurements were made in 50 mM MOPS (pH 7.0), 0.1 M KCl, 1 mM $MgCl_2$, 1 mM EGTA, and sufficient calcium chloride standard to yield the desired free calcium levels, which were initially estimated by use of the program MaxChelator and subsequently verified by use of ratiometric calcium-sensitive dyes Fura-2, Fura-4, and Fura-6, as previously described (*20*, *28*).

RESULTS

Calcium-Dependent Regulation of RyR1. The calcium dependence of the regulation of the RyR1 calcium release channel was measured from the binding of [^{3}H]-ryanodine to RyR1 in the absence and presence of bound CaM (Figure 2). These measurements used a heavy sarcoplasmic reticulum (HSR) fraction isolated from rat hind limb skeletal muscle and enriched in RyR1. The absence of bound CaM in this preparation was assessed by immunoblotting with antibodies against CaM and indicates <0.2 pmol of CaM/mg of SR protein (data not shown). Thus, it is possible to measure the calcium dependence of channel open probability in the absence of significant amounts of bound CaM (see below).

Ryanodine, which binds specifically to the open state of RyR, provides a functional measure of channel open probability and permits a determination of RyR1 abundance (*29*). At low calcium levels, associated with resting muscle (i.e., ~0.1 μM), [^{3}H]-ryanodine does not bind to RyR1, indicating that the channel is closed. A progressive increase in the fraction of open channels upon increasing the free calcium concentration is observed, with maximal [^{3}H]-ryanodine binding (i.e., 11 pmol/mg) between 10 and 100 μM free calcium. At higher calcium concentrations the [^{3}H]-ryanodine binding is decreased, consistent with prior observations for RyR1 isolated from rabbit muscle (*5*). The substantially larger abundance of RyR1 relative to any endogenous bound CaM in this SR preparation indicates that the observed calcium-dependent regulation is an inherent property of RyR1, consistent with prior suggestions that RyR1 contains EF-hand-like calcium binding sites (*30*). Thus, the RyR1 calcium release channel senses calcium levels to regulate its function independent of bound CaM, such that the initial release of calcium functions as a feedback activator of channel opening, and higher calcium levels function as feedback inhibitors of channel activity.

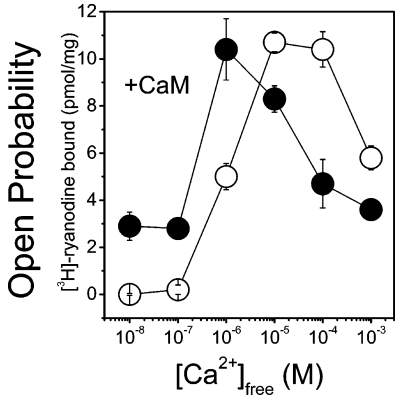

FIGURE 2: Calcium dependence of open channel probability. [^{3}H]-ryanodine binding to RyR1 was measured in heavy SR (120 μg/mL) prepared from rat hind limb skeletal muscle in the absence (○) or presence (●) of 250 nM CaM in 50 mM MOPS (pH 7.4), 300 mM NaCl, 100 μg/mL BSA, 0.1% CHAPS, 20 nM [^{3}H]-ryanodine, 0.7 mM EGTA, and sufficient $CaCl_2$ for the indicated free calcium concentrations. Ryanodine binding was assayed as described under Experimental Procedures. Average values and standard errors of the means are shown from measurements on three different preparations.

CaM-Dependent Regulation of RyR1. Addition of saturating amounts of CaM (i.e., 250 nM) increases the fraction of open channels at resting calcium levels and shifts the calcium dependence of channel opening to lower calcium concentrations, with maximal [^{3}H]-ryanodine binding occurring at approximately 1 μM free calcium, essentially as reported for the more commonly assayed rabbit RyR1 (*5*). Further, upon CaM association with RyR1, the calcium dependence of channel inactivation is shifted by 2 orders of magnitude toward lower calcium levels, functioning to enhance the calcium sensitivity of RyR1 to provide enhanced regulation within the physiological range of calcium levels associated with muscle contraction. Thus, CaM association functions to adjust the inherent calcium sensitivity of RyR1 channel open probability, serving as an activator at nanomolar free calcium concentrations and as an inhibitor at higher micromolar calcium levels.

Altered Conformation of CaM-Binding Sequence of RyR1 in Association with CaM. CaM binding to a peptide (i.e., RyRp) corresponding to the CaM-binding sequence (i.e., K^{3614}−N^{3643}) of RyR1 was measured through changes in the fluorescence intensity and mobility of the single Trp^{3620} within the CaM-binding sequence, permitting a determination of both binding affinity and calcium-dependent structural changes that may underlie the functional regulation of RyR. In the absence of CaM, the Trp fluorescence spectrum for RyRp is centered near 355 nm, consistent with the expected

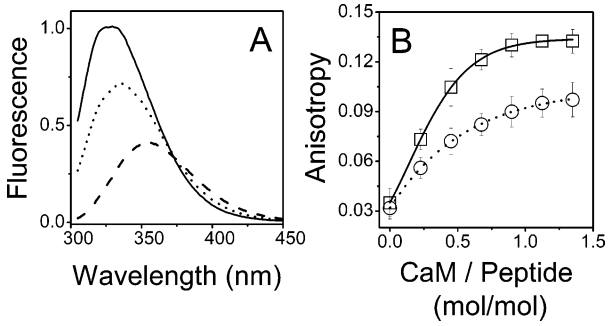

FIGURE 3: Calcium binding to CaM induces conformational changes within the CaM-binding sequence RyRp of the RyR1 calcium channel. Fluorescence spectra (A) and anisotropies (B) of Trp^{3620} within RyRp (1.1 μM) were measured alone (---) or following addition of 1.5 μM CaM at low (5 nM, ••• (○)) or activating (700 μM, — (□)) calcium levels in 50 mM MOPS (pH 7.0), 0.1 M KCl, 1 mM $MgCl_2$, and 1 mM EGTA in the absence or presence of 1.7 mM $CaCl_2$. Spectra were normalized to spectra of RyRp bound to calcium-activated CaM. For all measurements, $\lambda_{ex} = 295$ nm; for anisotropy measurements $\lambda_{em} = 350$ nm.

solvation of the highly exposed Trp^{3620} by water in the unbound peptide (Figure 3). Upon CaM binding, there are substantial increases in fluorescence intensity and the emission maximum is blue-shifted, consistent with the association between CaM (which lacks any tryptophans) and Trp^{3620} that is apparent in the crystal structure of calcium-activated CaM bound to RyRp (2BCX) (*13*). The bound conformation of RyRp is calcium-dependent, as is apparent from the large differences in the fluorescence emission spectra of apo-CaM and calcium-activated CaM bound to RyRp, that respectively induce 75% and 250% increases in fluorescence intensities and 19 or 27 nm blue shifts in the emission spectra of Trp^{3620} in RyRp (Figure 3A).

The structural interaction between CaM and RyRp is also apparent from a consideration of the rotational mobility of Trp^{3620}, which functions as a hydrophobic anchor in binding the C-domain of calcium-activated CaM (*13*). Upon CaM binding, the anisotropy of Trp^{3620} increases from 0.03 (essentially isotropic rotational motion) to either 0.10 (apo-CaM) or 0.13 (calcium-activated CaM) (Figure 3B), where a maximum value of 0.4 is indicative of no motion on the ns timescale. The large increase in anisotropy indicates a large decrease in the rotational mobility of Trp^{3620} upon CaM binding. Both apo-CaM and calcium-activated CaM associate with high affinity, as is apparent from the fact that binding is complete at a molar stoichiometry of 1 CaM/RyRp irrespective of calcium activation. The larger anisotropy associated with binding calcium-activated CaM in comparison to apo-CaM suggests a tighter binding interaction with Trp^{3620} and is consistent with prior measurements indicating that calcium binding induces structural changes within the complex between CaM and RyRp (*15*).

Individual Domains of Calcium-Activated CaM Bind with High Affinity to the CaM-Binding Sequence of RyR1. Calcium binding sites in the C-domain of CaM have higher affinities in comparison to the N-domain sites, and their preferential occupancy disrupts interdomain interactions to facilitate target protein binding (*20*, *23*, *31*−*34*). Furthermore, calcium-dependent differences in the affinities of the individual domains in CaM for RyRp have been suggested to underlie aspects of the CaM-dependent regulation of RyR1 (*7*, *13*, *17*). Therefore, to directly measure possible differences in

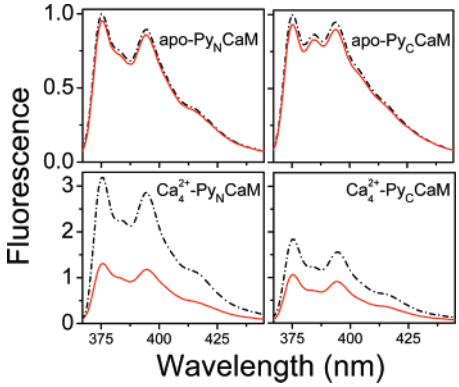

FIGURE 4: Sensitivities of Py_N- and Py_C-CaM sensors to RyRp binding. Fluorescence emission spectra of Py_N-CaM (left panels) or Py_C-CaM (right panels) at low (5 nM) (top panels) or high (700 μM) (lower panels) free calcium levels for CaM alone (black broken lines) or in the presence of 130 nM RyRp (red solid lines) for 100 nM CaM in 50 mM MOPS (pH 7.0), 0.1 M KCl, 1 mM $MgCl_2$, 1 mM EGTA, and sufficient $CaCl_2$ to yield the indicated free calcium levels. Spectra were normalized to F_{max} of the corresponding calcium CaM without peptide. $\lambda_{ex} = 330$ nm.

binding affinities, we have utilized *N*-(1-pyrene)maleimide to label two genetically engineered CaM mutants with unique cysteines either at position 110 (Py_C-CaM), within the C-terminal domain, or at position 34 (Py_N-CaM), within the N-terminal globular domain (Figure 1). We have previously demonstrated that associated fluorescence changes at these sites accurately reflect the differential calcium affinities of each globular domain of CaM in solution and that pyrene labeling at these sites does not perturb calcium binding or interaction with target proteins (*20*).

Upon binding of RyRp to either Py_N-CaM or Py_C-CaM, there is a decrease in fluorescence intensity in response to conformational rearrangements that alter the polar environment around the pyrene probes (Figure 4). A small (i.e., about 5%) decrease in fluorescence intensity occurs upon association of apo-CaM with RyRp (Figure 4), suggesting minimal structural changes upon binding. However, upon association of calcium-activated Py_N-CaM or Py_C-CaM with RyRp, much larger decreases in fluorescence are observed, corresponding a reduction of 55% and 42% of the integrated intensities. These observations are consistent with observed changes in charge density around sites of pyrene attachment in the high-resolution structures (see Figure S2). Specifically, both pyrene labeling sites in CaM are proximal to basic amino acids Arg^{3629} and Arg^{3630} in RyRp in the high-resolution structure of the CaM-bound complex 2BCX (*13*), whose increased charge density is expected to reduce the fluorescence signals of these probes.

Observed structural changes within the N- and C-domains of calcium-activated CaM, as reported by Py_N- and Py_C-CaM fluorescence, saturate at a ratio of 1 RyRp/CaM (Figure 5), indicating that both domains of CaM bind with high affinity to RyRp. These results are consistent with the observed high-affinity association of both apo-CaM and calcium-activated CaM with Trp^{3620} in RyRp (Figure 3B), and indicate that, upon calcium activation, both domains of CaM bind with high affinity to the CaM-binding sequence in RyR1.

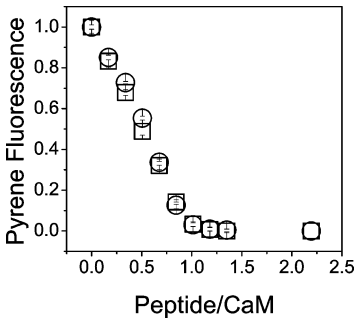

FIGURE 5: High-affinity binding of individual domains of calcium-activated CaM to RyRp. Decreases in fluorescence emission of Py_N-CaM (□) or Py_C-CaM (○) were measured upon addition of RyRp, for 100 nM CaM in 50 mM MOPS (pH 7.0), 0.1 M KCl, 1 mM $MgCl_2$, 1 mM EGTA, and 700 μM free calcium. The relative fluorescence is calculated as $[(F - F_{min})/(F_{max} - F_{min})]$. Symbols and error bars represent three independent measurements and the associated standard errors of the mean. Experimental conditions are as described in the caption for Figure 4.

Enhanced Calcium Affinities upon CaM Association with RyRp. Modulation of the calcium affinities of sites in CaM upon association with RyRp were measured via changes in the fluorescence of Py_N-CaM or Py_C-CaM. As previously described, calcium-dependent changes in the fluorescence of these sites accurately reflect calcium binding and associated conformational changes associated with CaM activation (*20*). Biphasic fluorescence changes are observed upon calcium activation of Py_C-CaM following binding to RyRp; that is, there is a decrease in fluorescence intensity upon increasing the calcium concentration from 2.0 to 400 nM (Figure 6), which is consistent with prior measurements indicating that the calcium affinity of CaM upon association with RyRp is in the nanomolar range (*16*, *35*). No corresponding changes in the fluorescence of Py_N-CaM are observed at submicromolar calcium levels, indicating that the observed fluorescence changes correspond to the calcium-dependent activation of the C-domain of CaM. The progressive decrease in Py_C-CaM fluorescence at these nanomolar calcium concentrations suggests that bound CaM undergoes conformational changes as calcium binds to the C-domain; these changes correlate with the activation of RyR1 at nanomolar calcium concentrations.

At higher calcium concentrations, there is a larger cooperative increase in the fluorescence intensity of Py_C-CaM with a half-point of 3.3 ± 0.4 μM, which is very similar to the calcium dependence of fluorescence changes for Py_N-CaM bound to RyRp ($[Ca]_{1/2} = 4.3 \pm 0.4$ μM). These latter results indicate a structural coupling between C- and N-terminal globular domains of CaM in the presence of RyRp, such that upon calcium binding to sites within the N-domain of CaM, concerted structural changes within the CaM−RyRp complex are sensed by both Py_C-CaM and Py_N-CaM. Furthermore, calcium-dependent structural changes sensed by both Py_C-CaM and Py_N-CaM coincide with the half-point of the calcium-dependent inhibition of the RyR1 calcium channel (Figures 1 and 6C), suggesting that calcium-induced structural changes associated with occupancy of sites in the N-domain of CaM contribute to the channel inhibition that occurs at micromolar calcium concentrations.

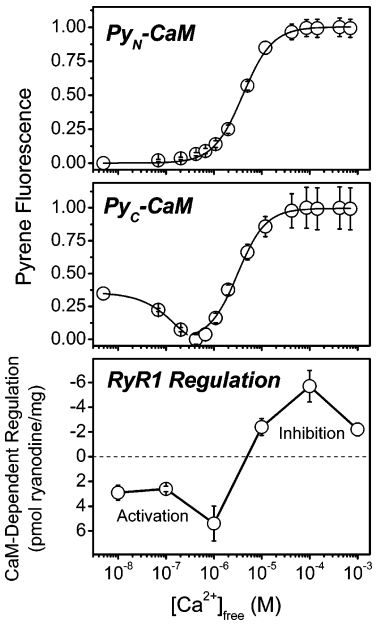

FIGURE 6: Calcium affinities of N- and C-terminal domains of CaM. Calcium-dependent changes in the relative fluorescence of either Py_N-CaM (upper panel) or Py_C-CaM (middle panel) were measured in the presence of saturating amounts of RyRp relative to observed CaM-dependent modulation of RyR1 channel function by CaM (lower panel; data taken from Figure 1). The relative fluorescence is calculated as $[(F - F_{min})/(F_{max} - F_{min})]$; CaM-dependent regulation is calculated as the ([^{3}H]-ryanodine binding in the presence of CaM) − ([^{3}H]-ryanodine binding in the absence of CaM). Experimental conditions involved CaM (100 nM) and RyRp (i.e., 130 nM) in 50 mM MOPS (pH 7.0), 0.1 M KCl, 1 mM $MgCl_2$, 1 mM EGTA, and sufficient $CaCl_2$ to yield the desired free calcium levels. Symbols and error bars represent three independent measurements and the associated standard errors of the mean. $\lambda_{ex} = 330$ nm; $\lambda_{em} = 375$ nm.

DISCUSSION

We find that structural changes associated with occupancy of N-domain calcium binding sites in CaM bound to the CaM-binding sequence of RyR1 (i.e., K^{3614}−N^{3643} or RyRp) induce structural changes within the CaM-binding sequence of RyR1, which were detected by use of mutants in which pyrene maleimides were incorporated onto either the C- or N-domains of CaM (i.e., Py_C- and Py_N-CaM) (Figure 6). The calcium dependence of these structural changes detected by pyrene probes within both N- and C-domains of CaM matches that associated with the CaM-dependent functional inhibition of RyR1 channel open probability as measured by [^{3}H]-ryanodine binding ($[Ca]_{1/2} = 4.3 \pm 0.4$ μM) (Figures 1 and 5). These results suggest that the calcium-dependent activation of the N-domain of CaM is responsible for global structural changes within the CaM-binding sequence RyRp and the enhanced inhibition of RyR1 observed at micromolar calcium concentrations. These structural changes are detected by changes in the fluorescence of both Py_N-CaM and Py_C-CaM (Figure 6) and involve concerted structural changes mediated by changes in the structure of RyRp (Figure S1, Supporting Information). In contrast, the calcium-dependent activation of the C-domain of CaM, apparent from changes in Py_C-CaM fluorescence, which occurs in the submicromolar calcium concentration range, matches that associated with the calcium-dependent activation of RyR1 (Figure 6). Thus, these results suggest different roles for calcium binding to

the high-affinity C-terminal sites versus the lower-affinity N-terminal sites within CaM in modulation of the respective calcium sensitivities of both RyR1 channel activation and inhibition.

Calcium-Dependent Activation of CaM in Association with RyRp. In agreement with this study demonstrating high-affinity calcium binding to the C-domain of CaM, prior observations have also suggested that CaM binding to a peptide corresponding to the RyR1 sequence $K^{3614}-N^{3563}$ (i.e., RyRp) dramatically increases the calcium affinity of CaM, with reported dissociation constants that vary between 81 ± 1 and 200 ± 100 nM (*15*, *16*). These prior observations were interpreted to suggest that the identified CaM-binding sequence is insufficient to explain the CaM-dependent regulation of RyR1, as calcium activation of CaM would occur at free calcium levels below 0.2 μM, which is close to that of resting muscle. Thus, the absence of a signal detecting physiologically relevant micromolar calcium-induced conformational changes of CaM suggested that additional CaM-binding, possibly noncontiguous, sites within RyR1 were necessary to explain the CaM-dependent regulation of RyR1 in muscle (*15*−*17*, *36*). As these prior measurements did not utilize sensitive probes capable of monitoring conformational events within each individual globular domain of CaM, domain-specific mechanisms related to the biphasic regulation of the RyR1 calcium channel were not resolved.

Thus, a critical element of this study is the sensitivity of pyrene fluorescence to its local environment along with its incorporation into CaM at sites 34 and 110 in the N- and C-domains (i.e., Py_N-CaM and Py_C-CaM), which has allowed individual measurements of calcium binding to and activation of either of the globular domains in CaM, without perturbation of normal calcium binding or target protein association (*20*). Indeed, the function and calcium binding affinities of pyrene-labeled CaM samples used in this paper are essentially identical to that associated with wild-type CaM. There is no change in the calcium concentration associated with half-maximal enzyme activation (*20*). The affinities of pyrene-labeled CaM are identical to that of unlabeled CaM for RyRp (Figures 3 and 5). Furthermore, the measured macroscopic dissociation constants (i.e., 1.2 μM and 5.2 μM) for pyrene-labeled CaM are in quantitative agreement with earlier measurements for unlabeled CaM, which for N- and C-terminal sites were respectively reported to be between 1 and 2 μM and 5−70 μM (*20*, *37*, *38*). Measurements of the high calcium-binding affinity for CaM in complex with RyRp reported in this paper ($[Ca]_{1/2} = 0.1-0.4$ μM free calcium) are in agreement with prior measurements of unlabeled CaM bound to RyRp (*15*, *16*, *20*). These results, coupled with the positions of the engineered sites associated with pyrene attachment that ensure no steric interference with CaM binding to RyRp (Figure 1), indicate that the measured calcium-dependent structural changes involving the complex between CaM and RyRp are not significantly affected by the presence of the bound pyrene probes.

Py_C-CaM and Py_N-CaM respectively sense distinct structural rearrangements within each globular domain of CaM bound to RyRp that correspond to the high-affinity calcium binding in the C-domain associated with channel activation (i.e., $[Ca]_{1/2} = 50$ nM), and the lower affinity calcium binding to the N-domain sites that are responsible for channel inhibition (i.e., $[Ca]_{1/2} = 4.3 \pm 0.4$ μM) (Figure 6). As a complementary measurement, the fluorescence changes of Trp^{3620} within RyRp were used to measure peptide binding to CaM; high-resolution structural analysis has demonstrated that Trp^{3620} associates with the C-terminal domain of CaM (Figure 2) (*13*). From Trp fluorescence changes, we observe a similar high-affinity binding of both apo-CaM and calcium-activated CaM to RyRp (Figure 3B). Likewise, changes in the fluorescence of Py_C- or Py_N-CaM indicate that both C- and N-domains bind with high affinity to RyRp following calcium activation (Figure 5). However, there are no significant fluorescence changes for Py_N-CaM upon association of apo-CaM with RyRp, making it uncertain whether the N-domain of CaM binds prior to calcium activation (Figure 4). Indeed, it has previously been suggested that, prior to calcium activation, the N-domain of CaM does not interact with the RyRp sequence but rather binds other sites on adjacent RyR1 subunits (*13*, *17*).

Structural Changes in the C-Domain of CaM in Association with RyRp. Calcium binding to the C-terminal globular domain of CaM has previously been implicated as critical to RyR1 channel inhibition (*35*, *36*). Consistent with this suggestion, we observe calcium-induced structural changes detected by changes in the fluorescence of Py_C-CaM in association with RyRp between 4 and 400 nM free calcium concentrations (Figure 6). These measurements are consistent with previously observed fluorescence changes in the complex between CaM and RyRp, which were detected by use of either acrylodan-labeled CaM or fluorescence changes associated with Trp^{3620} (*15*, *16*). Thus, the high-affinity binding of calcium to the C-domain of CaM bound to the RyR1 peptide results in detectable conformational transitions associated with domain activation. Calcium-dependent conformational changes involving only the C-domain are essentially complete near resting calcium levels ($\sim$0.1 μM) in the myocyte, which corresponds to the activation state of the RyR1 calcium channel (Figure 6). Thus, occupancy of calcium sites within the C-terminal domain of CaM bound to RyR1 induces structural changes that function to enhance a basal leak through the channel. These results support a role for the partial calcium occupancy of CaM, that is, CaM with two calcium ions bound in the C-domain and a calcium-free N-domain as an important species in the regulation of RyR1, consistent with the regulation of several other targets, including the SK channel and the anthrax edema factor (*39*, *40*). Supporting our conclusion that occupancy of calcium binding sites I and II in the N-domain of CaM represents the switch from activator to inhibitor of RyR1, B12Q, a CaM mutant for which these N-terminal calcium binding sites are disabled, can activate but not fully inhibit RyR1. On the other hand, the C-terminal analogue, B34Q, with calcium binding sites III and IV inactivated, is not able to properly activate or inhibit RyR1 (*35*).

N-Domain of CaM and Its Role in Modulating RyR1 Function. Our results indicate that calcium binding to the N-terminal domain of CaM induces global structural changes in the complex between CaM and RyRp, with a calcium dependence that mirrors that of the inhibition of the RyR1 channel and strongly suggests that CaM binding to the RyRp sequence is sufficient to explain calcium-dependent changes in the sensitivities of the complex between RyR1 and CaM (Figure 6). Thus, increases in cytosolic calcium during

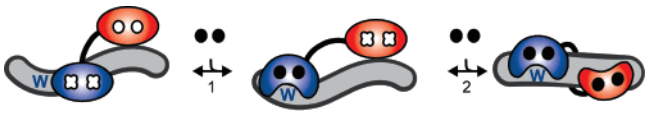

FIGURE 7: Model depicting calcium-dependent changes in the structure of the CaM in complex with RyRp. Calcium-dependent changes in the association between CaM and RyRp (gray) involve the sequential occupancy of calcium-binding sites in the C-domain (blue) (step 1) and N-domain (red) (step 2) of CaM that are associated with tertiary structural changes, with respective half-points at 0.2 and 4.3 μM free calcium concentrations that correlate with the calcium dependence of RyR1 channel regulation (see Figure 2). Association with both domains of CaM induces a structural change within RyRp (see Figure S1 in Supporting Information). Trp^{3620} (W) within RyRp functions as a hydrophobic anchor that associates with the calcium-activated C-domain of CaM (*13*). (●) Calcium ions.

muscle contraction lead to occupancy of calcium binding sites in the N-domain in addition to the calcium already bound to the C-domain of CaM. N-domain calcium binding induces global conformational changes that involve changes in the secondary structure of RyRp (Figure S1), such that both C- and N-domains respond with the formation of a productive high-affinity inhibitory complex with the RyR1 calcium channel. This end point has been characterized in detail with a high-resolution crystal structure of Ca_4−CaM in complex with RyRp, which reveals a collapsed CaM structure around the RyRp, reminiscent of those of classical CaM-binding sequences (e.g., MLCK and CaM-dependent protein kinase) (*14*, *41*, *42*), in which C- and N-domains of CaM bind at hydrophobic anchor residues, i.e., Trp^{3620} and Phe^{3636} on RyRp (*13*).

Conclusions and Future Directions. In summary, the differential calcium affinities observed for the C- and N-domains of CaM bound to the linear CaM-binding sequence in RyR1 are sufficient to explain the CaM-dependent regulation of RyR1 (Figure 7). Thus we propose that, at the low calcium levels associated with resting muscle, the C-terminal globular domain of CaM, with calcium sites III and IV occupied, is tethered to the CaM-binding sequence of RyR1. This close association provides a means to modulate the calcium sensitivity of the channel by positioning a conformationally sensitive calcium sensor, i.e., CaM, such that as intracellular calcium levels increase, calcium binding to sites I and II within the N-domain induces global conformational changes that promote channel closure prior to the calcium resequestration leading to muscle relaxation. At resting calcium levels, the N-domain of CaM is not associated with the CaM-binding sequence K^{3614}−N^{3643} in RyR1 but may bind to a noncontiguous binding site, such as the proposed N-terminal binding sequence Ser^{1975}−Arg^{1999} on an adjacent subunit of RyR1 that may selectively interact with the N-domain in apo-CaM to modulate the structural coupling between RyR1 subunits in response to changes in cytosolic calcium levels (*17*). Future work should be aimed at identifying the nature of the structural changes underlying RyR1 regulation and the possible involvement of other binding sequences that may associate with the N-domain of apo-CaM in association with RyR1.

SUPPORTING INFORMATION AVAILABLE

CD and FTIR spectra showing structural changes in RyRp upon calcium binding to CaM (Figure S1) and depictions of electrostatic surfaces in CaM (Figure S2). This material is available free of charge via the Internet at http://pubs.acs.org.

REFERENCES

1. Balshaw, D. M., Xu, L., Yamaguchi, N., Pasek, D. A., and Meissner, G. (2001) Calmodulin binding and inhibition of cardiac muscle calcium release channel (ryanodine receptor), *J. Biol. Chem. 276*, 20144−20153.
2. Fruen, B. R., Bardy, J. M., Byrem, T. M., Strasburg, G. M., and Louis, C. F. (2000) Differential Ca^{2+} sensitivity of skeletal and cardiac muscle ryanodine receptors in the presence of calmodulin, *Am. J. Physiol. Cell Physiol. 279*, C724−733.
3. Moore, C. P., Rodney, G., Zhang, J. Z., Santacruz-Toloza, L., Strasburg, G., and Hamilton, S. L. (1999) Apocalmodulin and Ca^{2+} calmodulin bind to the same region on the skeletal muscle Ca^{2+} release channel, *Biochemistry 38*, 8532−8537.
4. Rodney, G. G., Williams, B. Y., Strasburg, G. M., Beckingham, K., and Hamilton, S. L. (2000) Regulation of RYR1 activity by Ca^{2+} and calmodulin, *Biochemistry 39*, 7807−7812.
5. Tripathy, A., Xu, L., Mann, G., and Meissner, G. (1995) Calmodulin activation and inhibition of skeletal muscle Ca^{2+} release channel (ryanodine receptor), *Biophys. J. 69*, 106−119.
6. Meissner, G. (1986) Evidence of a role for calmodulin in the regulation of calcium release from skeletal muscle sarcoplasmic reticulum, *Biochemistry 25*, 244−251.
7. Samso, M., and Wagenknecht, T. (2002) Apocalmodulin and Ca^{2+}-calmodulin bind to neighboring locations on the ryanodine receptor, *J. Biol. Chem. 277*, 1349−1353.
8. O'Connell, K. M., Yamaguchi, N., Meissner, G., and Dirksen, R. T. (2002) Calmodulin binding to the 3614−3643 region of RyR1 is not essential for excitation-contraction coupling in skeletal myotubes, *J. Gen. Physiol. 120*, 337−347.
9. Takeshima, H., Nishimura, S., Matsumoto, T., Ishida, H., Kangawa, K., Minamino, N., Matsuo, H., Ueda, M., Hanaoka, M., Hirose, T., et al. (1989) Primary structure and expression from complementary DNA of skeletal muscle ryanodine receptor, *Nature 339*, 439−445.
10. Yamaguchi, N., Xin, C., and Meissner, G. (2001) Identification of apocalmodulin and Ca^{2+}-calmodulin regulatory domain in skeletal muscle Ca^{2+} release channel, ryanodine receptor, *J. Biol. Chem. 276*, 22579−22585.
11. Yamaguchi, N., Xu, L., Pasek, D. A., Evans, K. E., Chen, S. R., and Meissner, G. (2005) Calmodulin regulation and identification of calmodulin binding region of type-3 ryanodine receptor calcium release channel, *Biochemistry 44*, 15074−15081.
12. Yamaguchi, N., Xu, L., Pasek, D. A., Evans, K. E., and Meissner, G. (2003) Molecular basis of calmodulin binding to cardiac muscle Ca^{2+} release channel (ryanodine receptor), *J. Biol. Chem. 278*, 23480−23486.
13. Maximciuc, A. A., Putkey, J. A., Shamoo, Y., and Mackenzie, K. R. (2006) Complex of calmodulin with a ryanodine receptor target reveals a novel, flexible binding mode, *Structure 14*, 1547−1556.
14. Meador, W. E., Means, A. R., and Quiocho, F. A. (1992) Target enzyme recognition by calmodulin: 2.4 A structure of a calmodulin-peptide complex, *Science 257*, 1251−1255.
15. Rodney, G. G., Moore, C. P., Williams, B. Y., Zhang, J. Z., Krol, J., Pedersen, S. E., and Hamilton, S. L. (2001) Calcium binding to calmodulin leads to an N-terminal shift in its binding site on the ryanodine receptor, *J. Biol. Chem. 276*, 2069−2074.
16. Fruen, B. R., Balog, E. M., Schafer, J., Nitu, F. R., Thomas, D. D., and Cornea, R. L. (2005) Direct detection of calmodulin tuning by ryanodine receptor channel targets using a Ca^{2+}-sensitive acrylodan-labeled calmodulin, *Biochemistry 44*, 278−284.
17. Zhang, H., Zhang, J. Z., Danila, C. I., and Hamilton, S. L. (2003) A noncontiguous, intersubunit binding site for calmodulin on the skeletal muscle Ca^{2+} release channel, *J. Biol. Chem. 278*, 8348−8355.
18. Kranz, J. K., Lee, E. K., Nairn, A. C., and Wand, A. J. (2002) A direct test of the reductionist approach to structural studies of calmodulin activity: relevance of peptide models of target proteins, *J. Biol. Chem. 277*, 16351−16354.
19. Yao, Y., and Squier, T. C. (1996) Variable conformation and dynamics of calmodulin complexed with peptides derived from the autoinhibitory domains of target proteins, *Biochemistry 35*, 6815−6827.

20. Boschek, C. B., Squier, T. C., and Bigelow, D. J. (2007) Disruption of interdomain interactions upon partial calcium occupancy of calmodulin, *Biochemistry 46*, 4580−4588.
21. Allen, M. W., Urbauer, R. J., Zaidi, A., Williams, T. D., Urbauer, J. L., and Johnson, C. K. (2004) Fluorescence labeling, purification, and immobilization of a double cysteine mutant calmodulin fusion protein for single-molecule experiments, *Anal. Biochem. 325*, 273−284.
22. Strasburg, G. M., Hogan, M., Birmachu, W., Thomas, D. D., and Louis, C. F. (1988) Site-specific derivatives of wheat germ calmodulin. Interactions with troponin and sarcoplasmic reticulum, *J. Biol. Chem. 263*, 542−548.
23. Yin, D., Sun, H., Ferrington, D. A., and Squier, T. C. (2000) Closer proximity between opposing domains of vertebrate calmodulin following deletion of Met^{145}-Lys^{148}, *Biochemistry 39*, 10255−10268.
24. Mickelson, J. R., Ross, J. A., Reed, B. K., and Louis, C. F. (1986) Enhanced Ca^{2+}-induced calcium release by isolated sarcoplasmic reticulum vesicles from malignant hyperthermia susceptible pig muscle, *Biochim. Biophys. Acta 862*, 318−328.
25. Yang, H. C., Reedy, M. M., Burke, C. L., and Strasburg, G. M. (1994) Calmodulin interaction with the skeletal muscle sarcoplasmic reticulum calcium channel protein, *Biochemistry 33*, 518−525.
26. Zhang, J. Z., Wu, Y., Williams, B. Y., Rodney, G., Mandel, F., Strasburg, G. M., and Hamilton, S. L. (1999) Oxidation of the skeletal muscle Ca^{2+} release channel alters calmodulin binding, *Am. J. Physiol. 276*, C46−53.
27. Haugland, R. P., Ed. (2002) *Handbook of Fluorescent Probes and Research Products*, Molecular Probes, Inc., Eugene, OR.
28. Patton, C., Thompson, S., and Epel, D. (2004) Some precautions in using chelators to buffer metals in biological solutions, *Cell Calcium 35*, 427−431.
29. Pessah, I. N., Waterhouse, A. L., and Casida, J. E. (1985) The calcium-ryanodine receptor complex of skeletal and cardiac muscle, *Biochem. Biophys. Res. Commun. 128*, 449−456.
30. Fessenden, J. D., Feng, W., Pessah, I. N., and Allen, P. D. (2004) Mutational analysis of putative calcium binding motifs within the skeletal ryanodine receptor isoform, RyR1, *J. Biol. Chem. 279*, 53028−53035.
31. Kilhoffer, M. C., Lukas, T. J., Watterson, D. M., and Haiech, J. (1992) The heterodimer calmodulin: myosin light-chain kinase as a prototype vertebrate calcium signal transduction complex, *Biochim. Biophys. Acta 1160*, 8−15.
32. VanScyoc, W. S., Sorensen, B. R., Rusinova, E., Laws, W. R., Ross, J. B., and Shea, M. A. (2002) Calcium binding to calmodulin mutants monitored by domain-specific intrinsic phenylalanine and tyrosine fluorescence, *Biophys. J. 83*, 2767−2780.
33. Klevit, R. E., Dalgarno, D. C., Levine, B. A., and Williams, R. J. (1984) ^{1}H-NMR studies of calmodulin. The nature of the Ca^{2+}-dependent conformational change, *Eur. J. Biochem. 139*, 109−114.
34. Wang, C. L. (1985) A note on Ca^{2+} binding to calmodulin, *Biochem. Biophys. Res. Commun. 130*, 426−430.
35. Rodney, G. G., Krol, J., Williams, B., Beckingham, K., and Hamilton, S. L. (2001) The carboxy-terminal calcium binding sites of calmodulin control calmodulin's switch from an activator to an inhibitor of RYR1, *Biochemistry 40*, 12430−12435.
36. Xiong, L. W., Newman, R. A., Rodney, G. G., Thomas, O., Zhang, J. Z., Persechini, A., Shea, M. A., and Hamilton, S. L. (2002) Lobe-dependent regulation of ryanodine receptor type 1 by calmodulin, *J. Biol. Chem. 277*, 40862−40870.
37. Gilli, R., Lafitte, D., Lopez, C., Kilhoffer, M., Makarov, A., Briand, C., and Haiech, J. (1998) Thermodynamic analysis of calcium and magnesium binding to calmodulin, *Biochemistry 37*, 5450−5456.
38. VanScyoc, W. S., Newman, R. A., Sorensen, B. R., and Shea, M. A. (2006) Calcium binding to calmodulin mutants having domain-specific effects on the regulation of ion channels, *Biochemistry 45*, 14311−14324.
39. Drum, C. L., Yan, S. Z., Bard, J., Shen, Y. Q., Lu, D., Soelaiman, S., Grabarek, Z., Bohm, A., and Tang, W. J. (2002) Structural basis for the activation of anthrax adenylyl cyclase exotoxin by calmodulin, *Nature 415*, 396−402.
40. Schumacher, M. A., Rivard, A. F., Bachinger, H. P., and Adelman, J. P. (2001) Structure of the gating domain of a Ca^{2+}-activated K^+ channel complexed with Ca^{2+}/calmodulin, *Nature 410*, 1120−1124.
41. Ikura, M., Clore, G. M., Gronenborn, A. M., Zhu, G., Klee, C. B., and Bax, A. (1992) Solution structure of a calmodulin-target peptide complex by multidimensional NMR, *Science 256*, 632−638.
42. Meador, W. E., Means, A. R., and Quiocho, F. A. (1993) Modulation of calmodulin plasticity in molecular recognition on the basis of X-ray structures, *Science 262*, 1718−1721.

BI700655H